Implications of Sgr A* on the γ-rays searches of Bino Dark Matter with $(g-2)_\mu$

Utpal Chattopadhyay,
School of Physical Sciences,
Indian Association for the Cultivation of Science,
Kolkata, India

PASCOS-2025, Durham University, United Kingdom, July 21-25, 2025

JCAP (2025) 121, arXiv:2407.14603
(UC, D.Das, S. Poddar, R. Puri and A.K. Saha)

Outline:

- Bino-dominated lightest neutralino with slepton (and/or wino) coannihilation considered. This may satisfy the relic density as well as direct detection of DM constraints.
- Compressed SUSY. Low mass of the LSP as bino is generally difficult to detect at the LHC.
- The SUSY contributions to muon g-2 can be large for the above nature of LSP as bino. The effect due to the present scenario of the SM result.
- Typically with halo-only DM models, the indirect detection (via photon) prospect in the above case of SUSY falls far below the experimental thresholds from Fermi-LAT and HESS.
- A boost can be generated due to astrophysically dense objects like supermassive black hole (SMBH) like Sagittarius A^* near the galactic center.
- We assume DM exists. We will skip details of Minimal Supersymmetric standard model (MSSM).
- Brief description of DM density profile in presence of SMBH.
- Considering a few characteristic Benchmark points (BMP) we will analyze the effects on the SUSY parameter space.

Motivation:

- Signature of supersymmetry is yet to be seen at the LHC. However, there exists "compressed" SUSY scenarios with light superpartners which are still beyond the reach of the LHC. In "compressed" scenarios the mass gaps between certain superparticles can be small or very small. It would mean low KEs of decay products that are difficult to be distinguished from background. We will consider a SUSY model with bino type of lightest neutralino, the lightest supersymmetric particle (LSP). e.g. Slepton pair production and decay: $pp \to \tilde{l}^+\tilde{l}^- \to l^+\tilde{\chi}_1^0 l^-\tilde{\chi}_1^0 \Rightarrow l^+l^- \not{E}_T$.
- A relatively pure bino LSP can evade direct detection (relying on Higgs mediated effects).
- Relic Density of a light DM, as the sole candidate of DM can be satisfied only when certain conditions are fulfilled for DM self-annihilations and coannihilations. A Bino DM in general produces overabundance, but in certain situations like slepton-LSP coannihilation or bino-wino coannihilation it can be interesting while these fall in the compressed SUSY category.
- Indirect detection such as via photon signals may be explored since the rate is proportional to $\rho^2_{\rm DM}$ and this would be particularly enhanced for a strong gravitational potential like that is available around a Galactic Center (GC).

CONTINUED

Motivation: Bino dark matter, phenomenological status and prospects:

- A supermassive black hole (SMBH) Sagittarius A* (Sgr A*) at the GC has had time to possibly accrete DM in its proximity resulting into a "spike" with density $\rho_{\rm sp} >> \rho_{\rm DM}$, with ρ_{DM} referring to halo-only DM scenarios. The resulting denser DM profile largely dominated by $\rho_{\rm sp}$ may generate a large annihilation signal (Gondolo and Silk, 1999).
- In scenarios with light SUSY DM candidate, depending on the nature of DM candidate the intensity of signal can be too low in traditional halo-only DM based analyses in a BSM model like Minimal Supersymmetric Standard Model (MSSM). Typically, here the photon flux is a product of two separate quantities coming independently from particle physics and astrophysics inputs.

  We will consider a spiked DM environment around the supermassive black-hole Sgr A* located near the center of the Milky Way, and investigate the prospect of a boost that essentially does not allow factorization of the above particle and astrophysical parts for photon flux. We will probe a bino DM in relation to FERMI-LAT and HESS observations in two different energy domains.
- A light bino DM can produce large SUSY contributions to the anomalous magnetic moment of muon; $(g-2)_\mu$. In case of no deviation from SM, it would still put constraint on some parameters like $\tan\beta$.

Minimal Supersymmetric Standard Model (MSSM)

IN A NUTSHELL

- Supersymmetry (SUSY): A Boson-Fermion symmetry. It predicts fermionic and bosonic partners for SM bosons and fermions respectively. Equal masses of partners are not observed. SUSY must be a broken symmetry.
- MSSM Fields: SM fields added with Sfermion fields (scalars corresponding to SM fermions), Gauginos (fermions corresponding to SM bosons) and Higgsinos (fermions corresponding to Higgs scalars of SM in an extended Higgs setup).
- MSSM Lagrangian $\mathcal{L}_{\rm MSSM}$ consists of all gauge invariant parts such as i) SUSY preserving terms including SM Lagrangian, ii) SUSY preserving interactions involving SM fields and fields of SUSY partners satisfying certain conditions, and iii) soft SUSY breaking terms.
- Soft terms: Mass terms for superpartners of SM fields (bosonic and fermionic) and trilinear interaction of superpartner fields. These are called "soft" terms meaning they violate SUSY and produce only logarithmically divergent terms (i.e. no dangerous quadratic divergence of SM Higgs).

Gauge and Higgs Sectors:

Gauge Bosons	::	**Gauginos**
Gluons :	::	Gluinos
$G^a_\mu (a = 1 ... 8)$	::	$\widetilde{G}^a_\mu (a = 1 ... 8)$
Weak Bosons	::	Winos
$W^i_\mu (W^\pm, W^0)$	::	$(\widetilde{W}^\pm, \widetilde{W}^0)$
Abelian Boson(U(1))	::	Bino
B	::	$(\widetilde{B})$

Higgs bosons	::	**Higgsinos**
$H_U = \begin{pmatrix} H_U^+ \\ H_U^0 \end{pmatrix}$	::	$\widetilde{H}_U = \begin{pmatrix} \widetilde{H}_U^+ \\ \widetilde{H}_U^0 \end{pmatrix}$
$H_D = \begin{pmatrix} H_D^0 \\ H_D^- \end{pmatrix}$	::	$\widetilde{H}_D = \begin{pmatrix} \widetilde{H}_D^0 \\ \widetilde{H}_D^- \end{pmatrix}$

Gauginos are Majorona fermions (self-conjugate).

Charged Higgsinos are Dirac fermions and neutral ones are of Majorana type.

In SM, Electroweak Mixing: B and $W^0 \Rightarrow \gamma$ and Z.

In MSSM, Electroweak Mixing: $\widetilde{B}, \widetilde{W}^0, \widetilde{H}_U^0, \widetilde{H}_D^0 \Rightarrow$ Four neutralinos $(\tilde{\chi}_i^0)$

W^+, W^- (SM):: $\widetilde{W}^\pm, \widetilde{H}_U^+, \widetilde{H}_D^- \Rightarrow$ Two charginos $(\tilde{\chi}_i^\pm)$

With an extended Higgs sector compared to SM after EW symmetry breaking one has: 2 neutral CP-even Higgs h, H, 1 neutral CP-odd higgs (A-boson), 2 charged Higgs bosons ($H^\pm$); $\tan\beta = v_u/v_d$.

Gaugino and higgsino mixing: Neutralinos and Charginos

- Electroweak Symmetry Breaking $\Rightarrow$ mixing of gauginos and neutral higgsinos: $\tilde{B}, \tilde{W}_3, \tilde{H}_U^0, \tilde{H}_D^0 \Rightarrow$ 4 neutralinos $\tilde{\chi}_i^0$, $i = 1, 4$.

  The lightest one $\tilde{\chi}_1^0$ can be a DM candidate in R-parity preserving SUSY framework. R-parity is a discrete symmetry that avoids proton decay. It means superpartners are produced in pairs. Lightest SUSY particle is stable (LSP) since it cannot decay to another superpartner (DM candidate)

$$M_{\widetilde{\chi^0}} = \begin{pmatrix} M_1 & 0 & -M_Z \cos\beta \sin\theta_W & M_Z \sin\beta \sin\theta_W \\ 0 & M_2 & M_Z \cos\beta \cos\theta_W & -M_Z \sin\beta \cos\theta_W \\ -M_Z \cos\beta \sin\theta_W & M_Z \cos\beta \cos\theta_W & 0 & -\mu \\ M_Z \sin\beta \sin\theta_W & -M_Z \sin\beta \cos\theta_W & -\mu & 0 \end{pmatrix}.$$

- If μ and M_2 are large wrt M_1 the lightest neutralino $\tilde{\chi}_1^0$ is almost a bino whose interactions would involve $U(1)_Y$ gauge coupling g_1. Smaller μ or smaller M_2 would mean higgsino or wino like nature of $\tilde{\chi}_1^0$.
- Similarly, one has two charginos.

$$Charginos : M_{\widetilde{\chi^\pm}} = \begin{pmatrix} M_2 & \sqrt{2} M_W \sin\beta \\ \sqrt{2} M_W \cos\beta & \mu \end{pmatrix},$$

- If μ is large the lighter chargino $\tilde{\chi}_1^\pm$ would be wino-like in nature. Its interactions would be governed by gauge couplings. If μ is small the same will be higgsino-like whose interactions would be governed by Yukawa couplings.

Sfermion sector: Squarks, Sleptons and Sneutrinos

$$\textbf{Fermions} \iff \textbf{Sfermions}$$

$$Q_i : \begin{pmatrix} u \\ d \end{pmatrix}_L, \begin{pmatrix} c \\ s \end{pmatrix}_L, \begin{pmatrix} t \\ b \end{pmatrix}_L \iff \widetilde{Q}_i : \begin{pmatrix} \widetilde{u} \\ \widetilde{d} \end{pmatrix}_L, \begin{pmatrix} \widetilde{c} \\ \widetilde{s} \end{pmatrix}_L, \begin{pmatrix} \widetilde{t} \\ \widetilde{b} \end{pmatrix}_L$$

$$u_i : u_R, c_R, t_R \iff \widetilde{u}_i : \widetilde{u}_R, \widetilde{c}_R, \widetilde{t}_R$$

$$d_i : d_R, s_R, b_R \iff \widetilde{d}_i : \widetilde{d}_R, \widetilde{s}_R, \widetilde{b}_R$$

$$L_i : \begin{pmatrix} \nu_e \\ e \end{pmatrix}_L, \begin{pmatrix} \nu_\mu \\ \mu \end{pmatrix}_L, \begin{pmatrix} \nu_\tau \\ \tau \end{pmatrix}_L, \iff \widetilde{L}_i : \begin{pmatrix} \widetilde{\nu_e} \\ \widetilde{e} \end{pmatrix}_L, \begin{pmatrix} \widetilde{\nu_\mu} \\ \widetilde{\mu} \end{pmatrix}_L, \begin{pmatrix} \widetilde{\nu_\tau} \\ \tilde{\tau} \end{pmatrix}_L$$

$$e_i : e_R, \mu_R, \tau_R \iff \widetilde{e}_i : \widetilde{e}_R, \widetilde{\mu}_R, \tilde{\tau}_R$$

L and R tags for scalars are inherited from their fermionic partners.

There is no mixing in the sneutrino ($\tilde{\nu}$) sector since there is no right handed neutrino in SM.

- Mixing of scalar states namely squarks and sleptons.

$$M_{\tilde{t}}^2 = \begin{bmatrix} m_{\tilde{t}_L}^2 + (\frac{1}{2} - \frac{2}{3}\sin^2\theta_W)M_Z^2\cos 2\beta + m_t^2 & m_t(A_t - \mu\cot\beta) \\ m_t(A_t - \mu\cot\beta) & m_{\tilde{t}_R}^2 + \frac{2}{3}\sin^2\theta_W M_Z^2\cos 2\beta + m_t^2 \end{bmatrix},$$

$$M_{\tilde{e}}^2 = \begin{bmatrix} M_{\tilde{l_L}}{}^2 + (-\frac{1}{2} + \sin^2\theta_W)M_z^2\cos 2\beta + m_e^2 & m_e(A_e - \mu\tan\beta) \\ m_e(A_e - \mu\tan\beta) & M_{\tilde{l_R}}{}^2 - \sin^2\theta_W M_z^2\cos 2\beta + m_e^2 \end{bmatrix}.$$

$$M_{\tilde{\nu}}^2 = M_{\tilde{l_L}}{}^2 + \frac{1}{2}M_z^2\cos 2\beta$$

Relic density of a Bino dominated LSP

Typically a Bino dominated LSP ⇒ over-abundance of DM. Correct relic density is possible via i) Higgs mediation (h, H, A) in the s-channel, ii) Coannihilations: bino-wino and bino-slepton.

Higgsino and Wino dominated LSPs as solo DM candidates have LSP mass values at about 1 TeV and 2.5 TeV respectively. Low mass higgsino and wino are candidates for multi-component DMs (producing relic under-abundance).

Our relevant diagrams:

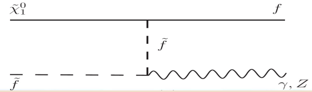

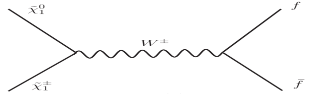

Direct detection of DM:
Neutralino-nucleon scattering and subsequent nuclear recoil. For small velocity scattering the following two terms are important.

$$\mathcal{L} = \alpha_{2i}\bar{\chi}\gamma^{\mu}\gamma^{5}\chi\bar{q}_i\gamma_{\mu}\gamma^{5}q_i + \alpha_{3i}\bar{\chi}\chi\bar{q}_i q_i$$

The DM neutralino $\tilde{\chi}_1^0$ that is almost a pure bino is prone to evade direct detection bounds from experiments like XENON1t etc. However, even a moderate amount of Higgsino mixing may not be allowed via the bounds.

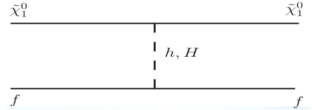

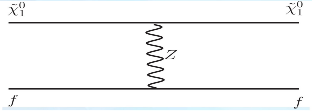

Anomalous magnetic moment of muon: $a_\mu = \frac{1}{2}(g-2)_\mu$

• The SM evaluation $a_\mu^{\rm SM}$ has the most challenging parts involving hadronic vacuum polarization and light by light diagrams. The old (2024)and present (2025) status of the deviation namely, $\delta a_\mu = a_\mu^{\rm exp} - a_\mu^{\rm SM}$ are widely different. The combined result of Fermilab and Broohaven Expts changed $a_\mu^{\rm exp}$ mildly, but $a_\mu^{\rm SM}$ varied significantly due to Lattice evaluations (Ref: arxiv: 2505.21476).

2024:
~~$\delta a_\mu = (249 \pm 49) \times 10^{-11}$~~;
~~$\delta a_\mu^{\rm BMW} = 107 \pm 69(\times 10^{-11})$~~,
~~$\delta a_\mu^{\rm CMD3} = 49 \pm 55(\times 10^{-11})$~~

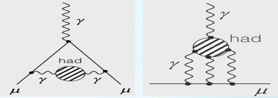

2025: (arxiv: 2505.21476)
$\delta a_\mu^{\rm present} = 26 \pm 66(\times 10^{-11})$

Because of similarity (no deviation from SM), our results labelled by $\delta a_\mu^{\rm CMD3}$ will be close to the situation of $\delta a_\mu^{\rm present}$.

SUSY: $a_\mu^{\rm SUSY} = \delta a_\mu$

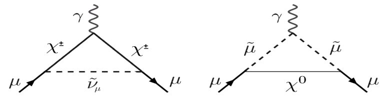

• The SUSY one-loops that contribute most are the ones with lighter chargino-sneutrino and lightest neutralino-smuon. $a_\mu^{\rm SUSY}$ receives larger SUSY contributions if the above particles are light.

• Light LSP as bino is a desired scenario for having a large $a_\mu^{\rm SUSY}$. Our Bino-DM SMBH photon signal analysis when seen in the the present $(g-2)_\mu$ scenario would allow the bino to be little more heavier. Also, $a_\mu^{\rm SUSY} \propto \tan\beta$ means $\tan\beta$ cannot be too large unless with heavier masses in the loop.

Dark Matter Density Profile Near the SMBH Sgr A*

- SMBH forms over time via accretion of matter as well as dark matter.
- DM particles are gravitationally attracted toward the SMBH giving rise to the DM density spike zone.
- DM annihilation in the dense region balances the spike formation. Thus the spike is flattened. However, the density remains much larger than the typical halo density outside the influence zone of the SMBH. A large DM density certainly enhances signals for indirect detection including that of photon signal.
- Halo region (outskirts of galaxy): $r > r_b$ with $r_b = GM/v_0^2$, v_0 being a non-relativistic velocity $\Rightarrow$ generalized Navarro-Frenk-White (NFW) distribution : $\rho(r) \sim r^{-\gamma_c}$.
- Spike region: $r_{\rm in} < r < r_b$, $\rho(r) \sim r^{-\gamma_{\rm sp}}$. One has $\gamma_{\rm sp} > \gamma_c$. $r_{\rm in}$ is defined via DM density for high annihilation region close to the SMBH competing with DM spike density.
- Annihilation Plateau ($4{\rm GM} < r \leq r_{in}$), where a spike gets flattened.
- Gravitational capture zone: $r < 4{\rm GM}$ when ρ vanishes.

Spike and halo DM density around Sgr A*.

- DM Halo: Outside r_b ($r > r_b$, DM halo zone): $\boxed{\rho(r) = \rho(r_b)(\frac{r_b}{r})^{\gamma_c}}$. The cusp parameter γ_c is obtained by numerical simulation. $\rho_b \equiv \rho(r_b)$ is found via DM density near the Sun $\boxed{\rho(r_b) = \rho_\odot(\frac{r_\odot}{r_b})^{\gamma_c}}$ $r_\odot = 8.46$ kpc, $\rho_\odot = \rho(r_\odot) = 0.3\ \mathrm{GeV/cm^3}$ Thus, $\boxed{\rho(r) = \rho_\odot(\frac{r_\odot}{r})^{\gamma_c}}$, where $r < r_\odot$. NFW profiles can approximately be given by a suitable γ_c.
- SMBH and DM: Actual DM density profile may differ from the above halo profile because of interplay between DM and the supermassive blackhole (SMBH) Sgr A*. A DM structure appreciably steeper than the cusp may be formed along with the growth of Sgr A* ($\tau \sim 10^{10}$ yrs) $\Rightarrow$ DM Spike.

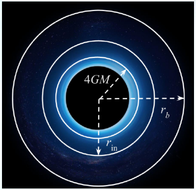

$M \equiv M_{\mathrm{BH}} = 4 \times 10^6 M_\odot$;
$\tau \sim 10^{10}$ years.
$r_b = \boxed{0.2\ \mathrm{pc}} \simeq 10^{17}\mathrm{cm}$,
$r_\odot = 8.46$ kpc.

$\boxed{r_b = GM/v_0^2}$,
with vel disp
$v_0 = 105\ \mathrm{km/s}$
$1\ \mathrm{pc} = 3.08 \times 10^{16}\mathrm{m}$

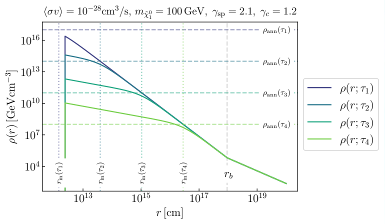

$r_\odot = 8.46$ kpc, $\rho_\odot = 0.3\ \mathrm{GeV/cm^3}$.

Spike and halo DM density around the Sgr A*.

- Spike zone: $r_{in} < r < r_b$: spike profile: $\rho_{\rm sp}(r) = \rho(r_b)(\frac{r_b}{r})^{\gamma_{\rm sp}}$. Unlike γ_c, $\gamma_{\rm sp}$ can be large and depends on formation history of the SMBH. For an adiabatic growth $\gamma_{\rm sp}^{\rm ad} = \left(\frac{9-2\gamma_c}{4-\gamma_c}\right)$ (Gondolo and Silk 1999). Essentially we will explore the effect of $\gamma_{\rm sp}$ in this work.
- Annihilation Plateau ($4{\rm GM} < r \leq r_{in}$): Annihilation plateau density $\rho_{\rm ann}(\tau) = m_{\tilde{\chi}_1^0}/\langle\sigma v\rangle\tau$ (Gondolo and Silk 1999). At time $\tau_{\rm in}$, $r_{\rm in} = r(\tau_{\rm in})$; profile dependence: $\rho_{\rm in}(r) = \rho_{\rm ann}(\tau_{\rm in}) \cdot (r_{\rm in}/r)^{\gamma_{\rm in}}$ (with typically $\gamma_{\rm in} = 0.5$). At $r = r_{\rm in}$, $\rho_{\rm in} = \rho_{\rm ann}$, At this critcal point: $\boxed{\rho_{\rm sp} \sim \rho_{\rm in} = \rho_{\rm ann}}$. $\rho_{\rm sp}$ and $\rho_{\rm in}$ will combine appropriately to give a smooth $\rho(r)$. The free rise of DM density due to $\rho_{\rm sp}$ for decreasing r becomes restricted for $r < r_{\rm in}$.
- For $r \lesssim 4{\rm GM}$ $\rho(r) = 0$ (Gravitational capture of BH).

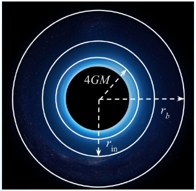

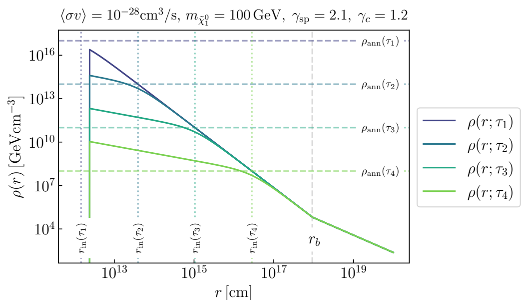

DM density around the Sgr A*.

- Spike zone: $r_{in} < r < r_b$: spike profile: $\rho_{\rm sp}(r) = \rho(r_b)(\frac{r_b}{r})^{\gamma_{\rm sp}}$.
- Annihilation Plateau ($4\mathrm{GM} < r \leq r_{in}$): $\rho_{\rm ann}(\tau) = m_{\tilde{\chi}_1^0}/\langle\sigma v\rangle\tau$.

  $\rho_{\rm in}(r) = \rho_{\rm ann}(\tau_{\rm in}) \cdot (r_{\rm in}/r)^{\gamma_{\rm in}}$.

$$\rho(r) = \begin{cases} 0 & (r < 4GM), \\ \dfrac{\rho_{\rm sp}(r)\rho_{\rm in}(r)}{\rho_{\rm sp}(r) + \rho_{\rm in}(r)} & (4GM \leq r \leq r_b), \\ \rho_b \left(\dfrac{r_b}{r}\right)^{\gamma_c} & (r_b < r \leq r_\odot), \end{cases}$$

Here, $r_b = GM/v_0^2$ and $\rho_b = \rho(r_b) = \rho_\odot(\frac{r_\odot}{r_b})^{\gamma_c}$. Both $\rho_{\rm sp}(r)$ and $\rho_{\rm in}(r)$ are decreasing functions of r. In $4GM \leq r \leq r_b$, if $\rho_{\rm in}(r)$ is large (i.e. small τ), $\rho(r) \simeq \rho_{\rm sp}(r)$. If $\rho_{\rm in}(r)$ small (large τ), $\rho(r) \simeq \rho_{\rm in}(r)$.

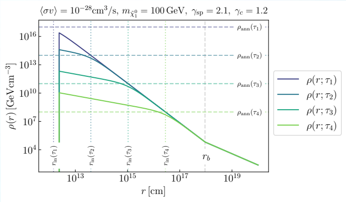

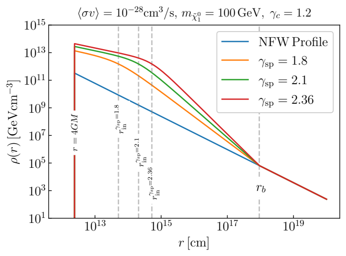

DM density for varying γ_c and $\gamma_{\rm sp}$.

$$\rho(r) = \begin{cases} 0 & (r < 4GM), \\ \dfrac{\rho_{\rm sp}(r)\rho_{\rm in}(r)}{\rho_{\rm sp}(r)+\rho_{\rm in}(r)} & (4GM \le r \le r_b), \\ \rho_b \left(\dfrac{r_b}{r}\right)^{\gamma_c} & (r_b < r \le r_\odot), \end{cases}$$

- Larger $\gamma_{\rm sp}$ $\Rightarrow$ steeper spike in the region $r_{\rm in} < r < r_b$.
- Larger γ_c $\Rightarrow$ Enhanced $\rho(r)$ in the entire region $4{\rm GM} < r < r_\odot$.

We use: $\gamma_c = 1.2$, which is the maximum allowed value from DM simulations, and we vary $\gamma_{\rm sp}$.

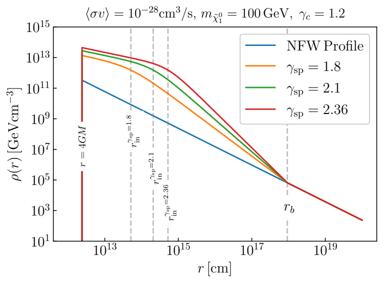

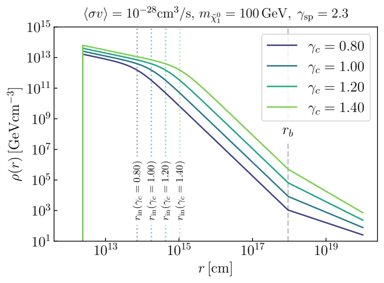

J-factor depends on $< \sigma v >$

Photon flux at Earth:

$$\frac{d\Phi}{dE_\gamma} = \frac{1}{4\pi} \frac{\langle \sigma v \rangle}{2m^2_{\tilde{\chi}^0_1}} \frac{dN}{dE_\gamma} \int_{\Delta\Omega} d\Omega \int_{\rm LOS} d\ell \, \rho^2_{\tilde{\chi}^0_1}(r)$$

$$= \frac{\langle \sigma v \rangle}{2m^2_{\tilde{\chi}^0_1}} \frac{dN}{dE_\gamma} \times J[\rho_{\tilde{\chi}^0_1}(r)]; \quad J[\rho_{\tilde{\chi}^0_1}(r)] = \frac{1}{r^2_\odot} \int_{4GM}^{r_b} \rho(r)^2 r^2 dr.$$

$\frac{dN}{dE_\gamma}$ is the differential photon spectrum per DM-DM annihilation.

For computing the line of sight (LOS) integral (over l) we note $r^2 = l^2 + r^2_\odot - 2lr_\odot \cos\psi$, Here $r_\odot$ is the Solar distance from the Galactic center, the included angle $\psi = 0$ at the Galactic center.

$$\frac{dN}{dE_\gamma} = \sum_i {\rm Br}(\tilde{\chi}^0_1 \, \tilde{\chi}^0_1 \to f_i) \, \frac{dN_i}{dE_\gamma}.$$

f_i refers to the final state particles in the ith annihilation channel.

For $(4{\rm GM} \leq r \leq r_b)$: $\rho_{\tilde{\chi}^0_1}(r) = \frac{\rho_{\rm sp}(r)\rho_{\rm in}(r)}{\rho_{\rm sp}(r) + \rho_{\rm in}(r)}$.

J-factor depends on $<\sigma v>$ (contd)

For $(4\mathrm{GM} \leq r \leq r_b)$: $\rho_{\tilde{\chi}_1^0}(r) = \dfrac{\rho_{\rm sp}(r)\rho_{\rm in}(r)}{\rho_{\rm sp}(r)+\rho_{\rm in}(r)}$.

• Thus, $\rho_{\tilde{\chi}_1^0}(r)$ depends on $<\sigma v>$ since, $\rho_{\rm in}(r) = \rho_{\rm ann}(\tau_{\rm in})\cdot(r_{\rm in}/r)^{\gamma_{\rm in}}$, where $\tau_{\rm in} = \tau(r_{\rm in})$, $\rho_{\rm ann}(\tau) = m_{\tilde{\chi}_1^0}/\langle\sigma v\rangle\tau \Rightarrow J$ decreases with τ except for the early time when it is quite flat.

• Presence of spike $\Rightarrow$ 3 to 6 order of magnitude enhancement of flux compared to the case of a halo-only DM profile.

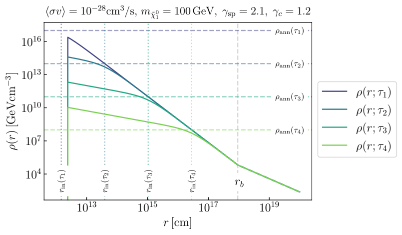

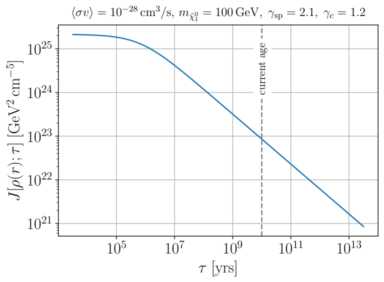

Differential Photon Flux in presence of a spike with J as a functional of $\rho(r)$.

$$\frac{d\Phi}{dE_\gamma} \simeq \frac{\langle \sigma v \rangle}{2m^2_{\tilde{\chi}^0_1}} \frac{dN}{dE_\gamma} \times J\left[\rho(r)\right].$$

- Unlike analyses with various halo-only DM profiles where J is segregated from particle physics inputs, here in presence of a spike around the SMBH J depends on $\langle \sigma v \rangle$.

Below: In the $m_{\tilde{\chi}^0_1} - \langle \sigma v \rangle$ plane J is shown as contours.

- Rise in J for low $\langle \sigma v \rangle$ and high DM mass.

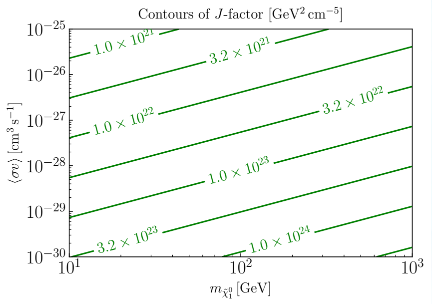

Dependence on halo profiles:

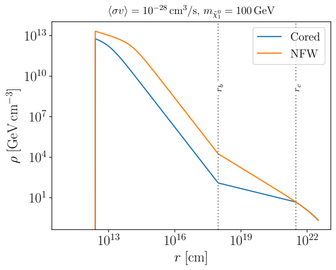

Spike profiles for cored ($\gamma_c = 0.4$, $r_c = 1$ kpc, $\gamma_{\rm sp} = 2.1$) and NFW ($\gamma_c = 1.2$, $\gamma_{\rm sp} = 2.1$).

Benchmark Points and Characteristics

	$\tilde{B}_{\tilde{H}}$			$\tilde{B}_{\tilde{W}\tilde{H}}$		
	BMP 1	BMP 2	BMP 3	BMP 4	BMP 5	BMP 6
M_1 [GeV]	200	300	350	200	300	600
M_2 [GeV]	1500	1500	1500	230	302	582
μ [GeV]	810	800	800	810	900	1200
$\tan\beta$	16	47	45	16	25	55
$m^{\rm in}_{\tilde{e}_L}, m^{\rm in}_{\tilde{e}_R}$ [GeV]	221	335	379	221	350	624
$m^{\rm in}_{\tilde{\mu}_L}, m^{\rm in}_{\tilde{\mu}_R}$ [GeV]	225	340	381	225	357	635
m_A	3000	4000	4000	3000	4000	4200
m_h [GeV]	122.7	123.3	123.3	123.6	123.8	123.7
$m_{\tilde{\chi}^0_1}$ [GeV]	199.4	300.3	350.5	199.40	300.4	603.5
$m_{\tilde{\chi}^0_2}$ [GeV]	831.9	829.5	829.1	241.2	323.0	618.5
$m_{\tilde{\chi}^\pm_1}$ [GeV]	831.7	829.2	828.6	245.3	323.1	618.4
$m_{\tilde{e}_R}$ [GeV]	206	303	351	206	319	606
$m_{\tilde{e}_L}$ [GeV]	244	363	405	239	373	643
$m_{\tilde{\mu}_R}$ [GeV]	210	308	353	210	327	617
$m_{\tilde{\mu}_L}$ [GeV]	248	369	407	243	380	655
$m_{\tilde{\nu}_e}$ [GeV]	231	354	397	226	364	638
$m_{\tilde{\nu}_\mu}$ [GeV]	235	359	399	230	371	649
${\rm Br}(B \to X_s\gamma) \times 10^4$	3.19	3.14	3.15	3.18	3.16	3.13
${\rm Br}(B^+ \to \tau^+\nu_\tau) \times 10^4$	1.25	1.24	1.24	1.24	1.24	1.24
${\rm Br}(B_s \to \mu^+\mu^-) \times 10^9$	3.17	3.13	3.13	3.17	3.17	3.11
${\rm Br}(B \to X_s\nu\bar{\nu}) \times 10^5$	3.98	3.98	3.98	3.98	3.98	3.98
$a^{\rm SUSY}_\mu \times 10^9$	1.77	2.14	1.59	2.82	1.94	1.51
$\Omega_{\rm DM}h^2$	0.119	0.122	0.121	0.121	0.119	0.118
$\sigma^p_{\rm SI}$ [pb] $\times 10^{11}$	2.40	3.77	5.46	2.95	4.16	8.88
$\langle\sigma_{\rm ann}v\rangle$ [cm^3/s] $\times 10^{28}$	0.95	1.19	1.30	1.08	1.31	1.73

Benchmark Points and Characteristics

	$\tilde{B}_{\tilde{H}}$			$\tilde{B}_{\tilde{W}\tilde{H}}$		
	BMP 1	BMP 2	BMP 3	BMP 4	BMP 5	BMP 6
M_1 [GeV]	200	300	350	200	300	600
M_2 [GeV]	1500	1500	1500	230	302	582
μ [GeV]	810	800	800	810	900	1200
$\tan\beta$	16	47	45	16	25	55
$m^{\rm in}_{\tilde{e}_L}, m^{\rm in}_{\tilde{e}_R}$ [GeV]	221	335	379	221	350	624
$m^{\rm in}_{\tilde{\mu}_L}, m^{\rm in}_{\tilde{\mu}_R}$ [GeV]	225	340	381	225	357	635
m_A [GeV]	3000	4000	4000	3000	4000	4200
$m_{\tilde{\chi}^0_1}$ [GeV]	199.4	300.3	350.5	199.4	300.4	603.5
$\Omega_{\rm DM}h^2$	0.119	0.122	0.121	0.121	0.119	0.118

- All six BMPs satisfy all the constraints from LHC, precision tests and, DM related data.
- Main constraints: $(g-2)_\mu$, (the 5σ deviation result), DM relic density, SI-DD and SD-DD cross-sections, and LHC-data (relaxed for a compressed scenario).
- Our task is to find the threshold value of the spike parameter $\gamma_{\rm sp}$ for a given BMP so that the photon signal just crosses the threshold detection abilities of FERMI-Lat and/or HESS experiments while satisfying other MSSM constraints. Then we extend the analysis to MSSM parameter space in general.

Benchmark Points and Characteristics

	$\tilde{B}_{\tilde{H}}$			$\tilde{B}_{\tilde{W}\tilde{H}}$		
	BMP 1	BMP 2	BMP 3	BMP 4	BMP 5	BMP 6
M_1 [GeV]	200	300	350	200	300	600
M_2 [GeV]	1500	1500	1500	230	302	582
μ [GeV]	810	800	800	810	900	1200
$\tan\beta$	16	47	45	16	25	55
$m^{\rm in}_{\tilde{e}_L}, m^{\rm in}_{\tilde{e}_R}$ [GeV]	221	335	379	221	350	624
$m^{\rm in}_{\tilde{\mu}_L}, m^{\rm in}_{\tilde{\mu}_R}$ [GeV]	225	340	381	225	357	635
m_A [GeV]	3000	4000	4000	3000	4000	4200
$m_{\tilde{\chi}^0_1}$ [GeV]	199.4	300.3	350.5	199.4	300.4	603.5
$\Omega_{\rm DM}h^2$	0.119	0.122	0.121	0.121	0.119	0.118

• BMP1 TO BMP3 under $B_{\tilde{H}}$: coannihilation with sleptons. $\tilde{\chi}^0_2$ and $\tilde{\chi}^0_3$ are dominated by Higgsinos with masses more than 800 GeV and decay to $\tilde{\chi}^0_1$ and h or Z boson.

• BMP4 TO BMP6 under $B_{\tilde{W}\tilde{H}}$: Coannihilation with lighter chargino and sleptons. $\tilde{\chi}^0_2$ is Wino-like with masses very close to $m_{\tilde{\chi}^0_1}$. BMP 5 is consistent with a three-body process via an off-shell W to $\tilde{\chi}^0_1, u(c), \overline{d}(\bar{s})$.
The BMPs refer to compressed spectra difficult for collider detections.

• $\langle \sigma v \rangle$ is not large enough to produce sufficient photon flux for Fermi-LAT and HESS under the halo-only DM profiles.

• To explore whether the presence of a DM spike around the SMBH Sgr A* can raise the cross-sections sufficiently.

Reach of $\langle \sigma v \rangle$ for photon spectra from different channels

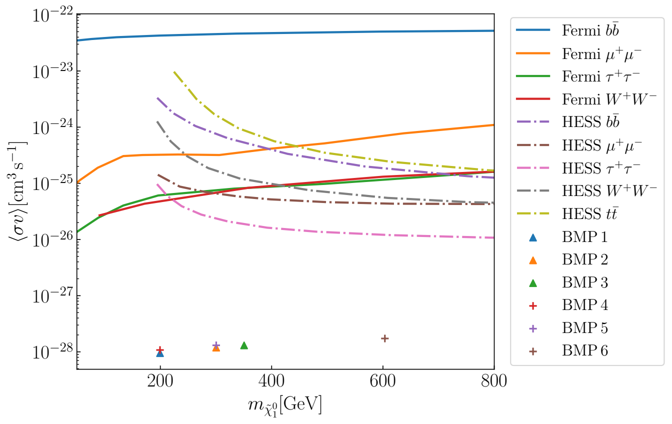

Comparison of total $\langle \sigma v \rangle$ values for BMP 1 - BMP 6 with experimental upper limits on DM pair annihilation cross-section to different final state particles. The Fermi-LAT upper bounds (for the NFW profile) to different final state particles assuming 100% branching ratio are from the observations of dSphs. The HESS bounds (for the Einasto profile) are from the observations of GC.

Dominant DM annihilation modes for BMPs of present era

$\tilde{B}_{\tilde{H}}$:

BMP 1 : $\tilde{\chi}_1^0\tilde{\chi}_1^0 \to \bar{t}t,\ \gamma e^+e^-,\ \gamma\mu^+\mu^-,$

BMP 2 : $\tilde{\chi}_1^0\tilde{\chi}_1^0 \to \bar{t}t,\ \gamma e^+e^-,\ \gamma\mu^+\mu^-,$

BMP 3 : $\tilde{\chi}_1^0\tilde{\chi}_1^0 \to \bar{t}t,\ \gamma e^+e^-,\ \gamma\mu^+\mu^-.$

$\tilde{B}_{\tilde{W}\tilde{H}}$:

BMP 4 : $\tilde{\chi}_1^0\tilde{\chi}_1^0 \to \bar{t}t,\ \gamma e^+e^-,\ \gamma\mu^+\mu^-,$

BMP 5 : $\tilde{\chi}_1^0\tilde{\chi}_1^0 \to \bar{t}t,\ W^+W^-,\ \gamma e^+e^-,$

BMP 6 : $\tilde{\chi}_1^0\tilde{\chi}_1^0 \to W^+W^-,\ \bar{t}t,\ b\bar{b}.$

- For quarks final states $\Rightarrow$ hadronization $\Rightarrow$ a large number of photons with varying energy.

- FSR diagrams are helicity suppressed ($\propto m_f$) unlike an Internal Bremsstrahlung (IB) diagram. In IB it is avoided at the expense of a QED effect of $\mathcal{O}(\alpha)$.

- For a bino LSP with close sfermion mass, the $\chi\chi \to f\bar{f}\gamma$ IB cross-section (3-body) becomes large via a logarithmic term (Bringmann, Bergstrom et al 2008 and earlier works). peaking at $\boxed{E_\gamma \simeq m_{\tilde{\chi}_1^0}}$. All our BMPs have masses $\geq$ 200, thus E_γ peaks fall in the HESS zone.

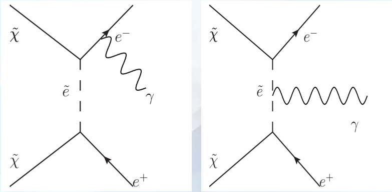

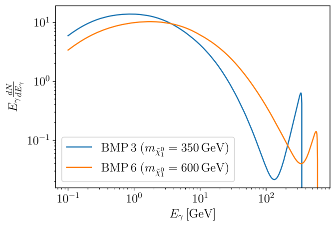

Comparing with Fermi-LAT and HESS data

$$(\Phi)_i = \int_{E^i_{\rm min}}^{E^i_{\rm max}} dE_\gamma \frac{d\Phi_\gamma}{dE_\gamma}; \qquad \frac{d\Phi}{dE_\gamma} \simeq \frac{\langle \sigma v \rangle}{2 m^2_{\tilde{\chi}^0_1}} \frac{dN}{dE_\gamma} \times J[\rho(r)],$$

where, ith bin's span $= E^i_{\rm max} - E^i_{\rm min}$, $\boxed{\frac{dN}{dE_\gamma} = \sum_i {\rm Br}(\tilde{\chi}^0_1 \tilde{\chi}^0_1 \to f_i)\, \frac{dN_i}{dE_\gamma}.}$

For all the BMPs and bins we compute:

$$\boxed{(E_{\rm med}\Phi)_i = \sqrt{E^i_{\rm min} E^i_{\rm max}} \int_{E^i_{\rm min}}^{E^i_{\rm max}} dE_\gamma \frac{d\Phi_\gamma}{dE_\gamma}}, \text{ where } (E_{\rm med})_i = \sqrt{E^i_{\rm min} E^i_{\rm max}}.$$

Energy flux values are computed at **each bin identical to those used in the Fermi-LAT and HESS data** for Sgr A*.

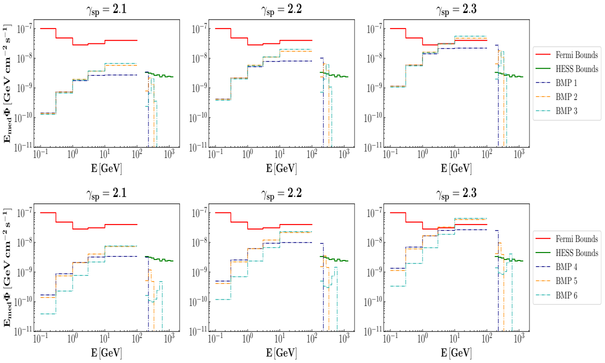

We use data from Fermi-LAT and HESS observation considering photon signal from Sgr A* for given spike parameters.
100 MeV $\leq E_\gamma \leq$ 100 GeV
180 GeV $\leq E_\gamma \leq$ 79 TeV

Photon spectra for BMP2 ($\in \tilde{B}_{\tilde{H}}$) except with varying μ

BMP2

M_1 [GeV]	300
M_2 [GeV]	1500
μ [GeV]	800
$\tan\beta$	47
$m^{\rm in}_{\tilde{e}_L}, m^{\rm in}_{\tilde{e}_R}$ [GeV]	335
$m^{\rm in}_{\tilde{\mu}_L}, m^{\rm in}_{\tilde{\mu}_R}$ [GeV]	340
m_A [GeV]	4000
$m_{\tilde{\chi}^0_1}$ [GeV]	300.3
$\Omega_{\rm DM} h^2$	0.122

- For final states with quarks $\Rightarrow$ hadronization $\Rightarrow$ large number of photons with low energy. dN_i/dE_γ peaks at a lower energy ($< m_{\tilde{\chi}^0_1}$); also true for channels with W-bosons.
- Leptonic final state channels have high energy photons with dN_i/dE_γ peaking near $< m_{\tilde{\chi}^0_1}$.
- Thus BMP1 to BMP3 will have two peaks with the prominent second peak for Internal Bremsstrahlung (IB) is covered by HESS.
- Low $\mu \Rightarrow$ Less bino in LSP $\Rightarrow$ Less IB or three body decay with photon. Hence with HESS that has $E_\gamma \geq 180$ GeV is effective.

BMP 2 : $\tilde{\chi}^0_1\tilde{\chi}^0_1 \to \bar{t}t,\ \gamma e^+e^-,\ \gamma\mu^+\mu^-$

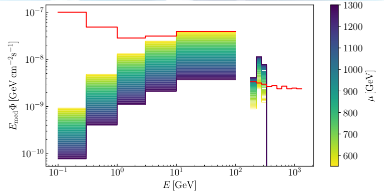

Varying μ; $\gamma_{\rm sp} = 2.2$ and $\gamma_c = 1.2$.
For smaller/larger μ values enhanced signals occur in lower/higher energies and are probed by Fermi-LAT/HESS expts.

BMP2 ($\in \tilde{B}_{\tilde{H}}$) with varying μ and/or $\tan\beta$: allowed regions:

- Top figure: Allowed region: White area between the two dashed lines for DM relic density.
- Points on the curved line refer to the maximum μ and $\gamma_{\rm sp}^{\rm min}$ values satisfying the photon signal constraints.
- Bottom figure:
  BMP2 with μ and $\tan\beta$ varying. Circles are color graded with the values of $\gamma_{\rm sp}^{\rm min}$.
- Regions above the CMD3 and BMW lines for δa_μ correspond to discarded zones via upper limit of $\tan\beta$.
- $\gamma_{\rm sp}^{\rm min}$ values are spread in a small range, irrespective of $\tan\beta$.

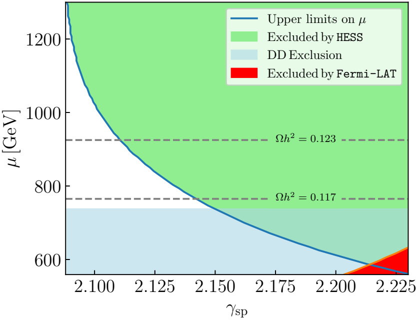

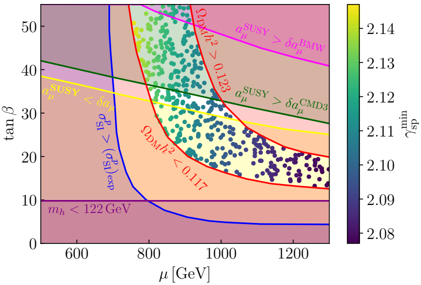

Photon spectra for BMP5 ($\tilde{B}_{\tilde{W}\tilde{H}}$): with varying μ and $\gamma_{\rm sp}$

- $M_2 \simeq M_1 \Rightarrow$ More low energy photons accessible to Fermi-LAT.
- With $M_2 \simeq M_1$, smaller μ values are likely to exceed SI-DD limits.
- Larger μ zones are likely to exceed the HESS bound even for smaller values of $\gamma_{\rm sp}$ due to IB enhancement.

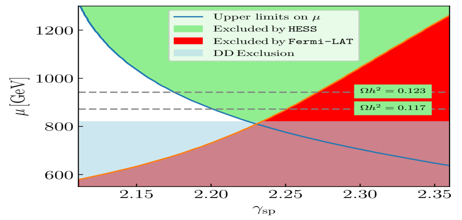

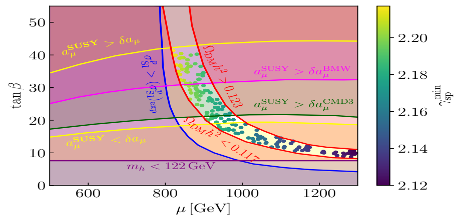

BMP5	
M_1 [GeV]	300
M_2 [GeV]	302
μ [GeV]	900
$\tan\beta$	25
$m^{\rm in}_{\tilde{e}_L}, m^{\rm in}_{\tilde{e}_R}$ [GeV]	350
$m^{\rm in}_{\tilde{\mu}_L}, m^{\rm in}_{\tilde{\mu}_R}$ [GeV]	357
m_A [GeV]	4000
$m_{\tilde{\chi}_1^0}$ [GeV]	300.4
$\Omega_{\rm DM}h^2$	0.119

BMP 5 : $\tilde{\chi}_1^0\tilde{\chi}_1^0 \to \bar{t}t,\ W^+W^-,\ \gamma e^+e^-$

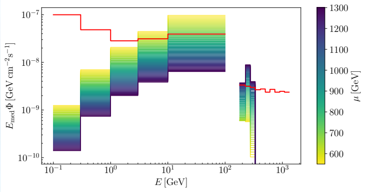

Photon spectra for BMP5: with varying M_2 and γ_{sp}

- Bino-wino-slepton all having similar masses mean lowering of DM relic density.
- BMP5: Larger M_2 regions are likely to exceed the HESS limit.
- Larger valid limit for γ_{sp}^{min}

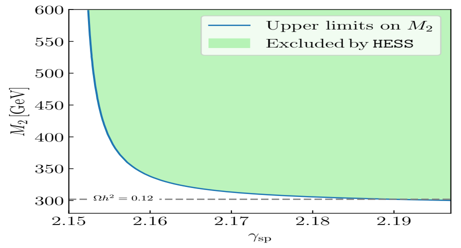

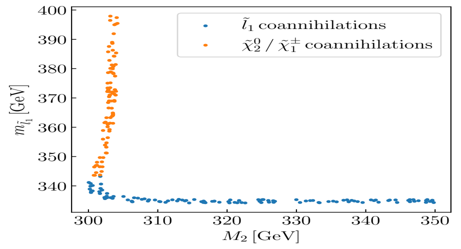

BMP5	
M_1 [GeV]	300
M_2 [GeV]	302
μ [GeV]	900
$\tan\beta$	25
$m_{\tilde{e}_L}^{in}, m_{\tilde{e}_R}^{in}$ [GeV]	350
$m_{\tilde{\mu}_L}^{in}, m_{\tilde{\mu}_R}^{in}$ [GeV]	357
m_A [GeV]	4000
$m_{\tilde{\chi}_1^0}$ [GeV]	300.4
$\Omega_{DM}h^2$	0.119

BMP 5 : $\tilde{\chi}_1^0\tilde{\chi}_1^0 \rightarrow \bar{t}t,\ W^+W^-,\ \gamma e^+e^-$

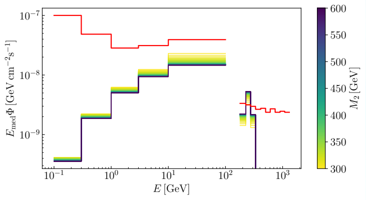

MSSM parameter scanning:

- Random scanning subject to preserving hierarchy of M_1, M_2 and μ such that the LSP remains to be bino-dominated in nature.
- All the constraints are applied including δa_μ with both new/old scenarios. The "CMD3" label is close to the present no deviation from SM picture.
- For each MSSM parameter point, $\gamma_{\rm sp}$ is varied to find $\gamma_{\rm sp}^{\rm min}$ via Fermi-LAT or HESS limits.
- Photon signal constraint is irrelevant if the LSP mass is in the 80 GeV gap region between the Fermi-LAT and HESS experiments. Especially the zone for IB effect will not be probed via HESS.

Bino-Higgsino :
$M_2 = 1.5$ TeV.

$$\begin{array}{rcccl} 100\,\mathrm{GeV} & \leq & M_1 & \leq & 700\,\mathrm{GeV}, \\ 2.0\,\mathrm{TeV} & \leq & M_A & \leq & 4.5\,\mathrm{TeV}, \\ 500\,\mathrm{GeV} & \leq & \mu & \leq & 1500\,\mathrm{GeV}, \\ 100\,\mathrm{GeV} & \leq & m_{\tilde{l}_{L,R}} & \leq & 1\,\mathrm{TeV}, \\ 5 & \leq & \tan\beta & \leq & 55. \end{array}$$

Bino-Wino-Higgsino :
M_2 is also being varied

$$\begin{array}{rcccl} 100\,\mathrm{GeV} & \leq & M_1 & \leq & 700\,\mathrm{GeV}, \\ 100\,\mathrm{GeV} & \leq & M_2 & \leq & 1\,\mathrm{TeV}, \\ 2.0\,\mathrm{TeV} & \leq & M_A & \leq & 4.5\,\mathrm{TeV}, \\ 500\,\mathrm{GeV} & \leq & \mu & \leq & 2.0\,\mathrm{TeV}, \\ 100\,\mathrm{GeV} & \leq & m_{\tilde{l}_{L,R}} & \leq & 1\,\mathrm{TeV}. \\ 5 & \leq & \tan\beta & \leq & 55, \end{array}$$

MSSM random scanning: Bino-Higgsino:

- Results with a small δa_μ limit (referred here as "CMD3").
- LSP mass is restricted within $200\,\mathrm{GeV} \lesssim m_{\tilde{\chi}_1^0} \lesssim 370\,\mathrm{GeV}$ beyond which one finds overabundant DM.
- Parameter regions with closely spaced slepton and LSP masses (compressed scenario). An allowed parameter point via photon signal (SMBH) constraint satisfies $\gamma_{\rm sp} < \gamma_{\rm sp}^{\rm min}$.

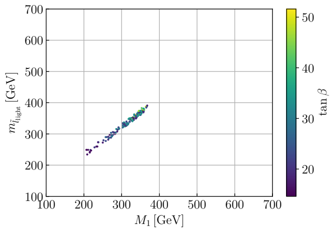

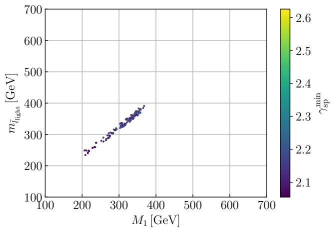

MSSM random scanning: Bino-Wino-Higgsino:

- Besides LSP-slepton, additionally there is LSP-lighter chargino coannihilations thus reducing the DM relic density.
- A broader allowed LSP mass range: $120\,\mathrm{GeV} \lesssim m_{\tilde{\chi}_1^0} \lesssim 700\,\mathrm{GeV}$.
- Irregularity of $\gamma_{\rm sp}^{\rm min}$ for $100 \lesssim M_1 \lesssim 275$ GeV is due to the 80 GeV gap between the Fermi-LAT ($E_\gamma \leq 100\,\mathrm{GeV}$) and the HESS ($E_\gamma \geq 180\,\mathrm{GeV}$) data. Additionally light bino, wino and slepton may potentially discard parameter points via δa_μ.
- An allowed parameter point via photon signal (SMBH) constraint satisfies $\gamma_{\rm sp} < \gamma_{\rm sp}^{\rm min}$.

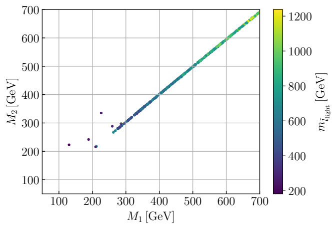

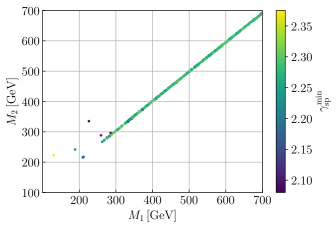

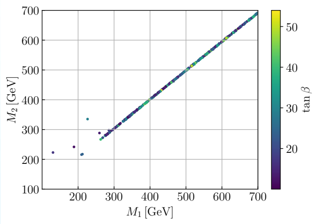

Bino-Wino-Higgsino with larger δa_μ:

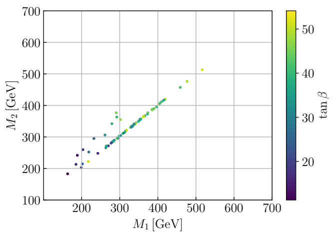

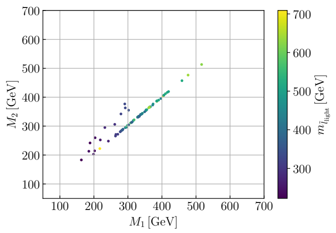

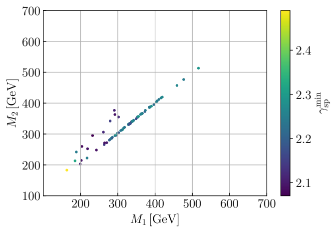

CONCLUSIONS

- Light bino dominated LSP in a bino-slepton or a bino-slepton-wino coannihilation scenario can simultaneously produce (i) the correct relic density, (ii) a compressed SUSY scenario, and (iii) it can also produce large SUSY contributions to $(g-2)_\mu$.
- With μ hardly too large, as in the BMPs the level of electroweak fine-tuning is also low.
- A bino dominated LSP can evade direct detection of DM limits because of too little higgsino mixing in it.
- On the other hand, a bino produces too little photon signals under halo-only DM profile scenarios.
- A supermassive blackhole like Sgr A* near the galactic center can have a spiked DM profile and this can enhance the photon signals so that a bino-LSP scenario can effectively be probed with appropriate values of the spike parameter.

BACKUP PAGES

Photon flux:

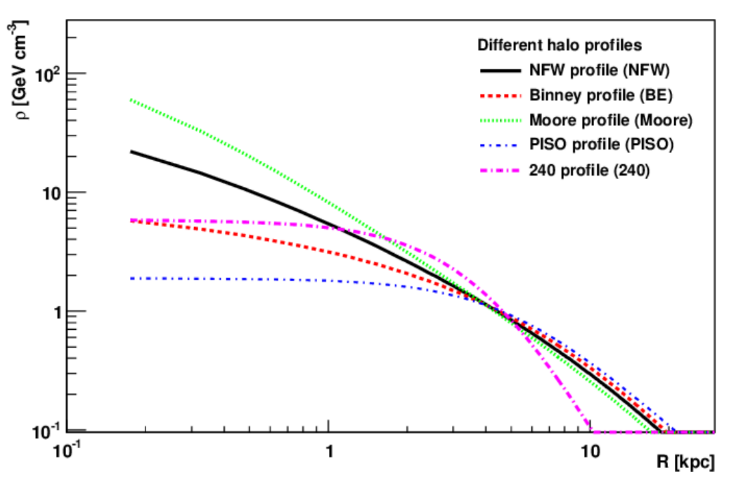
Different halo profiles
NFW profile (NFW)
Binney profile (BE)
Moore profile (Moore)
PISO profile (PISO)
240 profile (240)
ρ [GeV cm^-3]
10^2
10
1
10^-1
10^-1
1
10
R [kpc]

A few DM halo profiles:

Photon Flux from DM Annihilations

The annihilation rate in a small volume dV is given by:

$$d\Gamma = \sigma \times n_2 v_{\rm rel} \times n_1 dV$$

Averaging over velocity distribution and removing double counting of DM pairs,

$$d\Gamma = \langle \sigma_{\rm ann} v \rangle \frac{n^2(r)}{2} dV = \langle \sigma_{\rm ann} v \rangle \frac{\rho^2(r)}{2m_\chi^2}\, s^2\, d\Omega\, ds$$

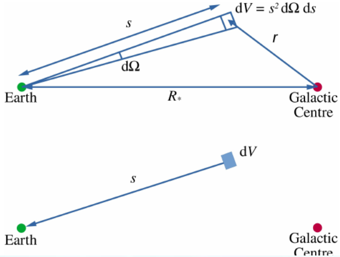

Photon spectrum at source:

$$d\left(\frac{dN}{dt\, dE_\gamma}\right) = \frac{dN}{dE_\gamma} \frac{\langle \sigma_{\rm ann} v \rangle}{2m_\chi^2} \rho^2(r)\, s^2\, d\Omega\, ds$$

Photon flux at earth:

$$\boxed{\frac{d\Phi}{dE_\gamma} = \frac{\langle \sigma_{\rm ann} v \rangle}{8\pi m_\chi^2} \frac{dN}{dE_\gamma} \int_{\Delta\Omega} d\Omega \int_{\rm LOS} \rho^2(r) ds}$$

MSSM

- The minimal supersymmetric standard model (MSSM) generalizes SM by including SUSY.
- The Lagrangian of MSSM consists of kinetic and gauge terms, terms derived from the superpotential W, and a softly broken supersymmetry part $\mathcal{L}_{soft}$.
- Superpotential W that preserves supersymmetry characterizes the theory. In terms of superfields one has:
  $W = \hat{U}\mathbf{Y_U}\hat{Q}\hat{H}_U - \hat{D}\mathbf{Y_D}\hat{Q}\hat{H}_D - \hat{E}\mathbf{Y_E}\hat{L}\hat{H}_D + \mu\hat{H}_U\hat{H}_D$
- The fields $\hat{U}$, $\hat{Q}$, $\hat{H}_U$ etc are chiral superfields that contain SM and superpartner fields. $\mathbf{Y_U}$, $\mathbf{Y_D}$ and $\mathbf{Y_E}$ are 3×3 Yukawa coupling matrices including all the generations of quarks and leptons.
- W is dominated by the third generation because of large top-quark mass.
- Unlike SM, SUSY requires two Higgs doublets H_U and H_D. This is due to holomorphicity of the superpotential, and anomaly cancellation requirements. With differing hypercharges H_U is associated with up type of squarks and H_D goes with leptons and down type of squarks.

MSSM, R-parity, and Dark Matter

$$W = \hat{U}\mathbf{Y_U}\hat{Q}\hat{H}_U - \hat{D}\mathbf{Y_D}\hat{Q}\hat{H}_D - \hat{E}\mathbf{Y_E}\hat{L}\hat{H}_D + \mu\hat{H}_U\hat{H}_D$$

- W refers to a version of SUSY that assumes R-parity to be conserved. $P_R = (-1)^{3(B-L)+2s}$. All SM particles have $P_R = 1$ and superpartners have $P_R = -1$.
- This means that superpartners are produced out of SM particles in pairs or a superpartner will decay into a superpartner along with an SM particle.
- $\Rightarrow$ The lightest supersymmetric particle (LSP) is stable.
- If neutral, the LSP may be a candidate for particle dark matter (DM).
- Typically lightest neutralino is a candidate for DM weakly interacting massive particle (WIMP).
- Conserved R-parity also avoids baryon and lepton number violations thus giving stability to proton.

MSSM

Superparticles need to be heavy ⇒ SUSY must be broken ⇒ we require $\mathcal{L}_{soft}$.
$\mathcal{L}_{soft}$ contains explicitly SUSY breaking terms that may have origin in a hidden sector based SUSY breaking framework. "Soft": because they will not cause any severe divergences due to renormalization except the mellowed logarithmic type of divergences.

$$
\begin{aligned}
-\mathcal{L}_{soft} &= \frac{1}{2}(M_3\bar{g}g + M_2\bar{W}W + M_1\bar{B}B + h.c.)\ \boxed{\text{gauginos}} \\
\boxed{\text{Trilinears}} \quad & +(\tilde{\bar{U}}\mathbf{a_U}\tilde{Q}H_U + \tilde{\bar{D}}\mathbf{a_D}\tilde{Q}H_D + \tilde{\bar{E}}\mathbf{a_E}\tilde{L}H_D + h.c.) \\
\boxed{\text{Masses}} \quad & +(\tilde{Q}^\dagger\mathbf{m_Q^2}\tilde{Q} + \tilde{L}^\dagger\mathbf{m_L^2}\tilde{L} + \tilde{\bar{U}}\mathbf{m_U^2}\tilde{\bar{U}}^\dagger + \tilde{\bar{E}}\mathbf{m_E^2}\tilde{\bar{E}}^\dagger) \\
& +m_{H_U}^2 H_U^* H_U + m_{H_D}^2 H_D^* H_D \\
\boxed{\text{Bilinear}} \quad & +(bH_U H_D + h.c.)
\end{aligned}
$$

$\mathcal{L}_{soft}$ has gauginos and scalars and but not their super-partners →violates supersymmetry.
$\mathbf{m^2}$: 3×3 Hermitian matrices in family space.
a: 3×3 trilinear coupling matrices: For convenience: $\mathbf{a} = \mathbf{AY}$. The version $\mathcal{L}_{soft}$ written here respects R-parity.
Large number of parameters for $\mathcal{L}_{soft}$.
Constraints from Flavor Changing Neutral Current (FCNC) and CP-violating effects strongly limit the parameters.

SUSY breaking terms and Electroweak Symmetry Breaking

- Two Higgs scalar doublet fields H_U and H_D with vacuum expectation values (VEVs) of their neutral components v_U and v_D. $\boxed{\tan\beta = \frac{v_U}{v_D}}$
- Neutral Higgs potential: $V_{Higgs} =$ $(\mu^2 + m^2_{H_U}) {H_U}^2 + (\mu^2 + m^2_{H_D}) {H_D}^2 - (b H_U H_D + h.c) + \frac{1}{8}(g^2 + g'^2)(H_U^2 - H_D^2)^2$
- Minimization conditions of V_{Higgs} at the EW scale:

$$\frac{1}{2} M_Z^2 = \underbrace{\frac{m^2_{H_D} - m^2_{H_U} \tan^2\beta}{\tan^2\beta - 1}}_{\text{SUSY breaking}} - \underbrace{\mu^2}_{\text{SUSY preserving}}$$

$$\sin 2\beta = \frac{2b}{(2\mu^2 + m^2_{H_U} + m^2_{H_D})}$$

- In constrained models (CMSSM/mSUGRA) with unification scale inputs, because of large m_t, RGE running of $m^2_{H_U}$ causes it to turn negative. Thus EW symmetry is broken radiatively rather than via an *ad hoc* negative mass-square term in the Higgs potential.
- μ problem: In spite of their different origins, the SUSY preserving μ parameter relates to SUSY breaking soft parameters. Various other SUSY models (NMSSM etc) are able to address this issue.

Electroweak Fine-Tuning

$$V = (m_{H_u}^2 + \mu^2)|H_u^0|^2 + (m_{H_d}^2 + \mu^2)|H_d^0|^2 - b(H_u^0 H_d^0 + h.c.) + \frac{1}{8}(g^2 + g'^2)(|H_u^0|^2 - |H_d^0|^2)^2$$

$$\boxed{\frac{M_Z^2}{2} = \underbrace{\frac{m_{H_d}^2 - m_{H_u}^2 \tan^2\beta}{\tan^2\beta - 1}}_{\text{SUSY Breaking}} - \underbrace{|\mu|^2}_{\text{SUSY Preserving}}}, \qquad \sin 2\beta = \frac{2b}{m_{H_d}^2 + m_{H_u}^2 + 2|\mu|^2}$$

Electroweak Fine-tuning Δ_{Total} *Perelstein and Spethmann,(JHEP-2007)* :

$$\Delta_{p_i} = \left| \frac{\partial \ln M_Z^2(p_i)}{\partial \ln p_i} \right|, \qquad \Delta_{Total} = \sqrt{\sum_i \Delta_{p_i}^2}, \text{where } p_i \equiv \{\mu^2, b, m_{H_u}, m_{H_d}\}$$

For valid $\tan\beta$ and μ zones $\boxed{\Delta_{Total} \simeq \Delta(\mu) \simeq \frac{4\mu^2}{m_Z^2}}$ $\Rightarrow$ **a small value of Δ_{Total} means a small value of μ.** A large μ would mean a cancellation of two large quantities requiring to produce a small quantity like $M_Z^2/2 \Rightarrow$ *unnatural* or finely-tuned scenario. The measure is inspired by Barbieri-Giudice's measure of fine-tuning where p_i refers to unification scale soft breaking input parameters. This is also close to μ^2/M_Z^2 of Chan, UC, P. Nath, PRD 1998.

Typically, a desirable SUSY spectra is the one with less fine-tuning in keeping with the motivation of SUSY.

Charged and Neutral Higgs Bosons

- There are two CP-even neutral Higgs bosons (h, H) out of which h has typically SM-like couplings, one pseudoscalar Higgs boson (A), and two charged Higgs bosons (H^+, H^-). Typically, all other Higgs bosons except h are quite heavy.
- With $X_t = A_t - \mu \cot\beta$, at one-loop: $m_h^2 \simeq M_Z^2 \cos^2(2\beta) + \Delta m_h^2$

$$\Delta m_h^2 = \frac{3 g_2^2 \bar{m}_t^4}{8\pi^2 {M_W}^2} \left[\ln\left(\frac{m_{\tilde{t}_1} m_{\tilde{t}_2}}{\bar{m}_t^2} \right) + \frac{X_t^2}{m_{\tilde{t}_1} m_{\tilde{t}_2}} \left(1 - \frac{X_t^2}{12 m_{\tilde{t}_1} m_{\tilde{t}_2}} \right) \right]$$

  Above its $(m_{h_{\rm tree}})$ tree level value near M_Z, a rather large amount of correction is needed to reach $m_h = 125$ GeV. Thus LHC forces us to have quite different levels of corrections from top-quark and top-squarks. $\Rightarrow$ Little hierarchy problem.
- A_t modulates m_h. It is remarkable that observed higgs mass is below the MSSM predicted upper limit of $m_h \lesssim 135$GeV.

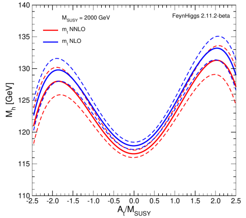

$[M_{\rm SUSY} = \sqrt{m_{\tilde{t}_1} m_{\tilde{t}_2}}]$; (Ref: Heinemeyer et. al. 2015)

Phenomenological MSSM (pMSSM)

- Simplifying scenario with CP-conservation and R-parity.

- Flavor: Minimal flavor violation with degenerate first two generations of sfermions (i.e. No more than CKM). These two generations are associated with small Yukawa couplings.

- 19 real parameters all given at a suitable Weak scale.
  Third generation inputs : $m_{Q_3}, m_{U_3}, m_{D_3}, m_{L_3}, m_{E_3}$;
  First two gens: $m_{Q_1}, m_{U_1}, m_{D_1}, m_{L_1}, m_{E_1}$;
  Third gen trilinears: A_t, A_b, A_τ; Gauginos: M_1, M_2, M_3;
  Higgsino/Higgs: μ, m_A and $\tan\beta$.

- Trilinears for the first two generations are zero. Additionally, all the non-diagonal entries of the mass parameters and trilinears are assumed to be zero.

Consequences of low energy SUSY: Example of Sparticle production:

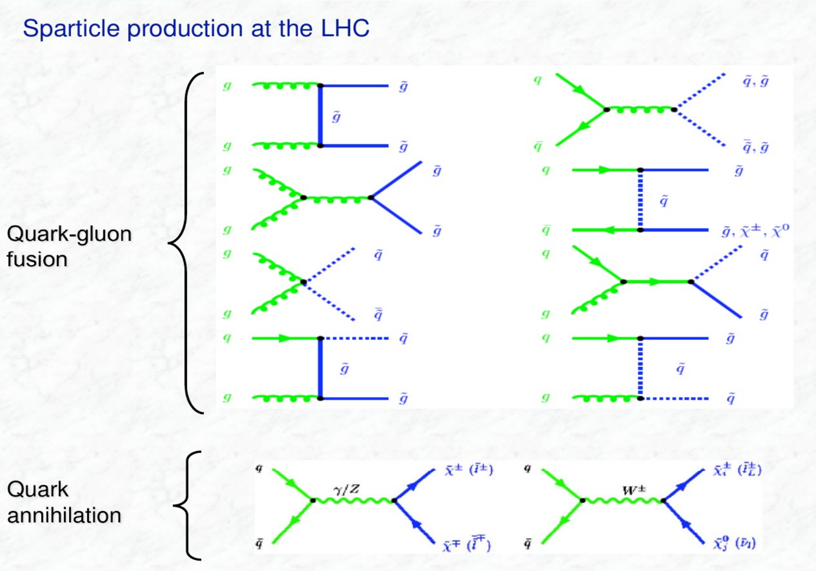

A clean SUSY Example: 3-lepton plus missing energy from $\tilde{\chi}_1^{\pm} - \tilde{\chi}_2^0$ pairs

- Decay via sleptons/sneutrinos:

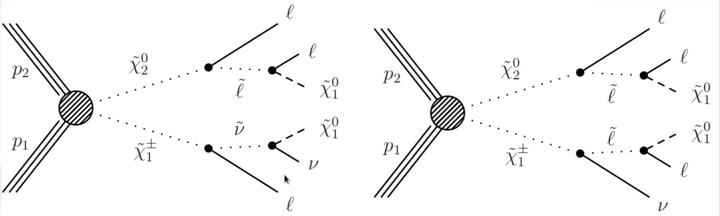

- Decay via gauge bosons leading to 3 leptons plus missing energy:

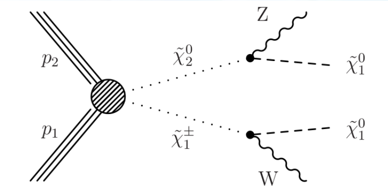

LHC (ATLAS limits):

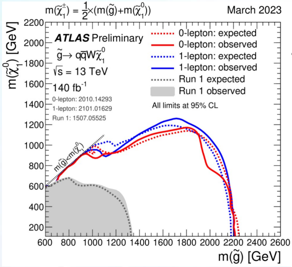

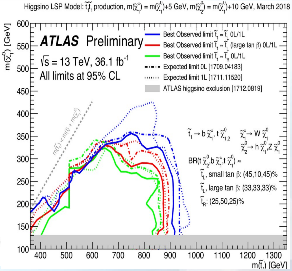

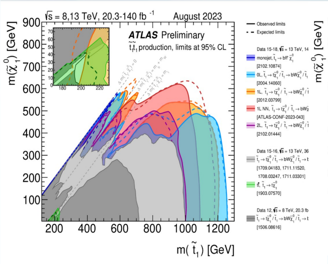

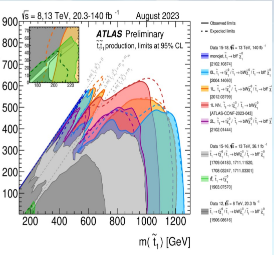

Specimen exclusions from ATLAS 2023 SUSY Searches limits

Direct detection of Dark Matter

- Direct detection relies on neutralino-nucleon scattering and subsequent nuclear recoil. For small velocity scattering the following two terms are important.

$$\mathcal{L} = \alpha_{2i}\bar{\chi}\gamma^{\mu}\gamma^{5}\chi\bar{q}_i\gamma_{\mu}\gamma^{5}q_i + \alpha_{3i}\bar{\chi}\chi\bar{q}_i q_i$$

- First and second terms: spin-dependent and spin-independent cross sections respectively. α_{2i} and α_{3i} are the appropriate couplings. The above is to be summed over the quark flavors. The subscript i labels up-type quarks ($i = 1$) and down-type quarks ($i = 2$).
- The scalar cross-section depends on t-channel Higgs exchange diagrams and the s-channel squark diagrams.
- Unless, the squark masses are close to the mass of the LSP, the Higgs exchange diagrams usually dominate over the s-channel diagrams.
- Spin-dependent cross section has t-channel Z exchange and s-channel squark exchange diagrams.

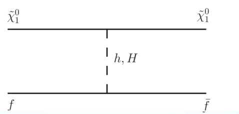

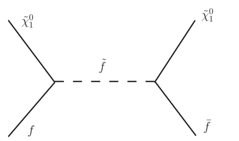

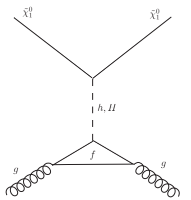

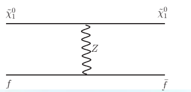

Anomalous magnetic moment of muon

g-factor for a lepton magnetic moment to spin. $\vec{\mu}_S = g_l \frac{e}{2m} \vec{S}$; $a_l = \frac{1}{2}(g_l - 2)$.
Large discrepancy from the SM (about 5σ):

$$a_\mu^{\mathrm{exp}} = 116\,592\,059\ (22) \times 10^{-11}; \quad a_\mu^{\mathrm{SM}} = 116\,591\,810\ (43) \times 10^{-11}$$

$$a_\mu^{\mathrm{exp}} - a_\mu^{SM} = (249 \pm 49) \times 10^{-11} \equiv a_\mu^{\mathrm{NewPhysics}}$$

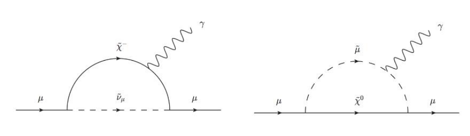

Simplified result in MSSM: When the loops that contribute most are the ones with lighter chargino-sneutrino and bino-smuon fields:

$$a_l^{\tilde{\chi}^\pm} \simeq \frac{\alpha_2\, m_l^2\, \mu\, M_2 \tan\beta}{4\pi \sin^2\theta_W\, m_{\tilde{\nu}_l}^2} \left(\frac{f_{\chi^\pm}(M_2^2/m_{\tilde{\nu}_l}^2) - f_{\chi^\pm}(l^2/m_{\tilde{\nu}_l}^2)}{M_2^2 - \mu^2} \right),$$

$$a_l^{\tilde{\chi}^0} \simeq \frac{\alpha_1\, m_l^2\ M_1(\mu\tan\beta - A_l)}{4\pi\cos^2\theta_W\,(m_{\tilde{l}_R}^2 - m_{\tilde{l}_L}^2)} \left(\frac{f_{\chi^0}(M_1^2/m_{\tilde{l}_R}^2)}{m_{\tilde{l}_R}^2} - \frac{f_{\chi^0}(M_1^2/m_{\tilde{l}_L}^2)}{m_{\tilde{l}_L}^2} \right).$$

Flavor Physics Constraint: $Br(b \to s\gamma)$

- $Br(b \to s\gamma)$ limits may put severe constraints on SUSY parameter space. The limits agree well with SM. Because of two Higgs doublets, MSSM is vulnerable for flavor constraints, but there can be suppression of MSSM contributions.

- At one-loop level MSSM diagrams include charged Higgs and charginos and these two contributions may add each other constructively or destructively depending on the signs of μ and A_t.

- The contribution from the charged Higgs boson (through the H^--t loop) exhibits the same sign and comparable magnitude when compared to the W^--t loop contribution of the SM, which already accounts for the experimental findings.

- $3.02 \times 10^{-4} < Br(b \to s\gamma) < 3.62 \times 10^{-4}$.

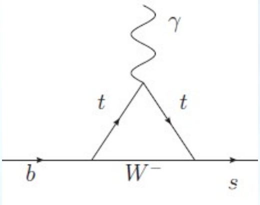

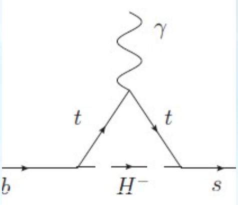

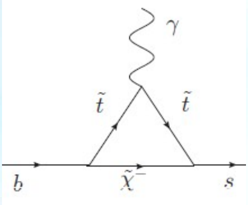

Anomalous magnetic moment of muon

Fermilab and Brookhaven: $a_\mu^{\rm exp} = 116\ 592\ 059\ (22) \times 10^{-11}$

$$\delta a_\mu \equiv a_\mu^{\rm exp} - a_\mu^{\rm SM} = (249 \pm 49) \times 10^{-11} \quad (5\sigma \text{ deviation})$$

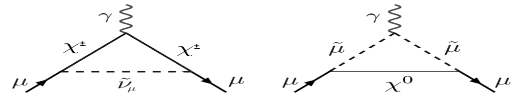

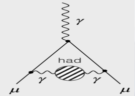

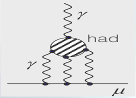

• There are large uncertainties in computing $a_\mu^{\rm SM}$ primarily due to hadronic vacuum polarization and light by light scattering diagrams.

• Two other evaluations of the diagrams alter $a_\mu^{\rm SM} \Rightarrow$

$\delta a_\mu^{\rm BMW} = 107 \pm 69 (\times 10^{-11})$ and, $\delta a_\mu^{\rm CMD3} = 49 \pm 55 (\times 10^{-11})$.

• $\delta a_\mu \equiv a_\mu^{\rm SUSY}$. The SUSY one-loops that contribute most are the ones with lighter chargino-sneutrino and bino-smuon fields. More contributions if the above particles are light. Also $a_\mu^{\rm SUSY} \propto \tan\beta$.

• We will choose a light bino type of neutralino ($\tilde{\chi}_1^0$) and light smuon scenario.

Dark matter : Rotation Curve of Galaxies

- Observed speed does not fall like $1/\sqrt{r}$ as expected from $v = \sqrt{\frac{GM}{r}}$, rather it is quite flat over the distance. This is even true for objects at the edge of galaxies. Thus $M \Rightarrow M(r) = 4\pi \int_0^r \rho(r')r'^2 dr'$, with $\rho(r') = 1/r'^2$ for flatness. $\Rightarrow$ Dark Matter (DM).
- Many candidates for DM. We focus on particle dark matter. Neutrinos $\Rightarrow$ hot DM. Structure formation issues may likely prefer cold dark matter (non-relativistic).
- Supersymmetry gives a candidate for DM that is a weakly interacting massive particle (WIMP). Apart from gravity, WIMPs may interact only by weak interaction.
- From Planck: DM: $\Omega_c h^2 = 0.112$, Baryons: $\Omega_b h^2 = 0.022$.

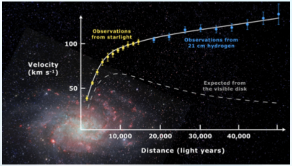

Rotation curve of spiral galaxy Messier 33

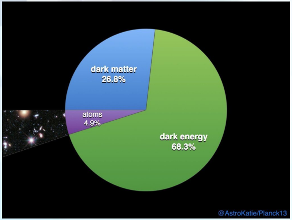

Bullet cluster: two colliding galaxy clusters

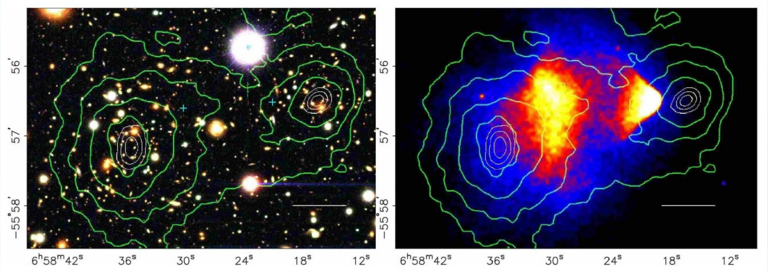

Figure: The distribution of the star components of the cluster along with mass density isocontours & the distribution of dust as seen in X-rays against mass density isocontours.

Gravitational lensing does not follow the baryonic matter but show strongest effects in two separated regions near the visible galaxies. ⇒ Existence of collisionless dark matter.

Thermal Equilibrium, Annihilation, Freeze-out and Relic density

- Thermal Equilibrium Era: ($T >> m_\chi$) in the early universe. Annihilation of χ's to SM particles and production of χ's from SM particles are similar $\Rightarrow$ Thermal equilibrium.
- Annihilation Era: ($T >> m_\chi/10$). Annihilation dominates since SM particles are not all that energetic to create χ's.
- Freeze-out Era: ($T \sim m_\chi/25$). Annihilation is ineffective because of dilution due to expansion of universe $\rightarrow$Relic abundance: $\Omega_\chi h^2 \sim \frac{3\times 10^{-27}}{<\sigma_{eff} v>}\ \mathrm{cm}^3/s$. Planck Data: $\Omega_\chi h^2 = 0.120 \pm 0.001$.
- One computes $<\sigma_{eff} v>$ where v is the relative velocity of two annihilating WIMPs. $<\sigma_{eff} v>$ is the annihilation cross-section to all final states.
- Coannihilation effects needs to be incorporated. This arises from annihilation of WIMP with another particle with nearly degenerate mass.

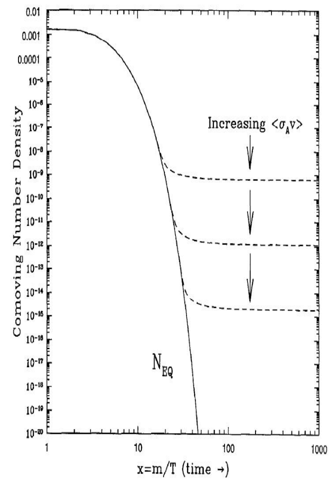

Neutralino Relic Density: $\Omega_\chi h^2$

One computes $< \sigma_{eff} v >$ by including LSP annihilation and co-annihilation processes.
Annihilation diagrams:

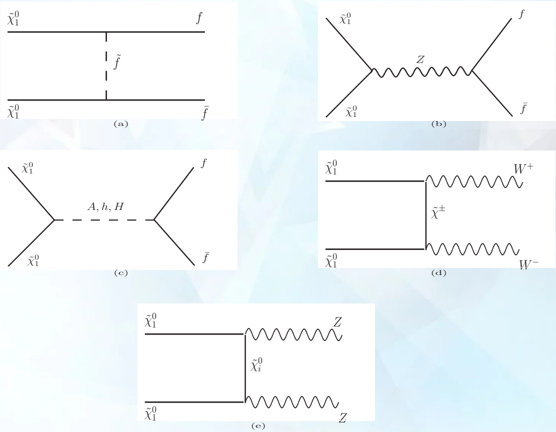

Figure 3.1: A few of the dominant neutralino annihilation diagrams.

72

Coannihilation Diagrams

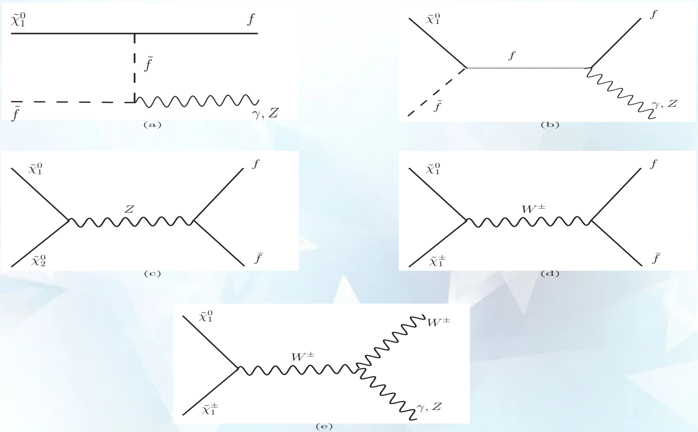

Figure 3.2: A few of the dominant neutralino coannihilation diagrams.

73

Nature of the lightest neutralino, either principally a bino, a wino or a higgsino as well as its mass determines $\Omega_\chi h^2$. PLANCK data: $\Omega_\chi h^2 = 0.120 \pm 0.001$. The above in turn constrains SUSY parameter space.